

# MONOTONICITY PROPERTIES OF BLOW-UP TIME FOR NONLINEAR SCHRÖDINGER EQUATION: NUMERICAL TESTS

CHRISTOPHE BESSE, RÉMI CARLES, NORBERT J. MAUSER,  
AND HANS PETER STIMMING

**ABSTRACT.** We consider the focusing nonlinear Schrödinger equation, in the  $L^2$ -critical and supercritical cases. We investigate numerically the dependence of the blow-up time on a parameter in three cases: dependence upon the coupling constant, when the initial data are fixed; dependence upon the strength of a quadratic oscillation in the initial data when the equation and the initial profile are fixed; finally, dependence upon a damping factor when the initial data are fixed. It turns out that in most situations monotonicity in the evolution of the blow-up time does not occur. In the case of quadratic oscillations in the initial data, with critical nonlinearity, monotonicity holds; this is proven analytically.

## 1. INTRODUCTION

Consider the Schrödinger equation with focusing nonlinearity  $(\lambda, \sigma > 0)$ :

$$(1.1) \quad i\partial_t u + \Delta u = -\lambda|u|^{2\sigma}u, \quad (t, x) \in \mathbb{R}_+ \times \mathbb{R}^n \quad ; \quad u|_{t=0} = u_0.$$

Such an equation may appear as an envelope equation in the propagation of lasers (see e.g. [28], and [10, 15] for a rigorous mathematical justification). It is well known that if  $u_0 \in H^1(\mathbb{R}^n)$  (inhomogeneous Sobolev space) and  $\sigma < \frac{2}{n-2}$ , then (1.1) has a unique solution in  $H^1(\mathbb{R}^n)$ , defined locally in time (see e.g. [8]). It needs not remain in  $H^1(\mathbb{R}^n)$  globally in time: finite time blow-up may occur when  $\sigma \geq \frac{2}{n}$  and  $\lambda > 0$  (focusing, or attractive, nonlinearity); see e.g. [6, 8, 28]. Since  $\lambda \in \mathbb{R}$ , the  $L^2$ -norm of  $u(t, \cdot)$  is independent of time, and finite time blow-up means that there exists  $T > 0$  (we consider only forward time evolution) such that:

$$\|\nabla_x u(t)\|_{L^2} \rightarrow +\infty \quad \text{as } t \rightarrow T.$$

Many papers provide important properties about the blow-up rate or the profile at blow-up; see e.g. [29, 30, 18, 19, 7, 22, 24, 20, 21, 26] for some analytical results, and [27] for a nice survey of the latest results. We also point out that recent numerical experiments [12] have shown a completely new phenomenon, where the blow-up profile is independent of the usual ground state (quasi self-similar ring profile), and the blow-up rate seems to be the minimal one given by the theory (square root blow-up rate). As recalled in

---

1991 *Mathematics Subject Classification.* [

This work was supported by the Austrian Ministry of Science (BM:BWK) via its grant for the Wolfgang Pauli Institute and by the Austrian Science Foundation (FWF) via the START Project (Y-137-TEC) and by the European network HYKE funded by the EC as contract HPRN-CT-2002-00282.

[27], the main three directions of research in this subject are: giving sufficient conditions to have finite time blow-up in the energy space; estimating the blow-up rate and the stability of the blow-up régimes; describing the spatial structure of the singularity formation. On the other hand, it seems little attention has been paid to the time where blow-up occurs. In this paper, we investigate by numerical experiments the dependence of the blow-up time upon, for instance, the coupling constant  $\lambda$ , when the initial datum  $u_0$  is fixed.

To motivate our study, we recall some results from [9] and [11]. In [9], the authors prove that if the initial datum  $u_0(x)$  is replaced by  $u_0(x)e^{-ib|x|^2/4}$ , then one can relate explicitly the blow-up time of the corresponding new solution  $u_b$  to that of  $u$ , in the case of a critical nonlinearity,  $\sigma = \frac{2}{n}$ . This is a consequence of the conformal invariance. In the super-critical case  $\sigma > \frac{2}{n}$ , the conformal transform does not leave (1.1) invariant, and introduces a factor  $(1 - bt)^{n\sigma-2}$  in front of the nonlinearity. It is also established in [9] that if  $u$  has negative energy (in this case, there is finite time blow-up at least if  $xu_0 \in L^2(\mathbb{R}^n)$  [14]; see also [23, 17] for weaker assumptions), then *for large  $b$* , blow-up occurs sooner than for  $b = 0$ ; unlike in the conformally invariant case, one does not know whether the blow-up time is monotonous with respect to  $b$ . The numerical experiments we present here show that it is not monotonous with respect to  $b$ .

In [11], the author considers the damped cubic Schrödinger in space dimension two:

$$(1.2) \quad i\partial_t \psi + \Delta \psi = -i\delta \psi - |\psi|^2 \psi, \quad (t, x) \in \mathbb{R}_+ \times \mathbb{R}^2 \quad ; \quad \psi|_{t=0} = u_0.$$

It is conjectured that the blow-up time is monotonous with respect to  $\delta > 0$ , and guessed that the same holds in the super-critical case. Our numerical experiments show that neither of the two guesses is satisfied. These two guesses are very satisfactory when one think of the initial datum  $u_0$  as a single hump; numerics also suggest that in this case, the blow-up time is monotonous with respect to  $\delta$ . On the other hand if  $u_0$  is made of, say, two humps, then the initial intuition seems to be wrong.

Note that introducing  $u(t, x) = e^{\delta t} \psi(t, x)$ , Equation (1.2) is equivalent to:

$$(1.3) \quad i\partial_t u + \Delta u = -e^{-2\delta t} |u|^2 u, \quad (t, x) \in \mathbb{R}_+ \times \mathbb{R}^2 \quad ; \quad u|_{t=0} = u_0.$$

As in the case of initial quadratic oscillations mentioned above, this transform yields an equation of the form (1.1), with a time-dependent coupling “constant”,  $\lambda = e^{-2\delta t}$ . This function of time is monotonous, decreasing.

This naturally leads us to the question, when  $\lambda$  is really a constant: is the blow-up time monotonous with respect to  $\lambda$ ? Tracking the dependence of the blow-up time upon  $\lambda$  can be viewed as both a generalization and a study case of the two problems raised in [9] and [11]. Numerics show that both in the critical ( $\sigma = \frac{2}{n}$ ) and in the supercritical case ( $\sigma > \frac{2}{n}$ ), one should not expect the blow-up time to be monotonous with respect to  $\lambda$ . Essentially, the idea is the same as what was announced above: when the initial datum  $u_0$  is a single Gaussian, then monotonicity seems to hold. When  $u_0$  is the superposition of two such functions, there is a lack of monotonicity.

Roughly speaking, suppose that two humps are placed to both sides of the origin and that the natural (free) time evolution tends to send mass from both these humps to the origin. This may occur thanks to a particular phase term, for instance, or simply mass dispersion. For large  $\lambda$ , the blow-up occurs before the two humps have merged: the two humps do not interact before the blow-up, and break down independently. For small  $\lambda$ , these humps merge into one hump before blow-up takes place. Asymptotically, for “large”  $\lambda$  or for “small”  $\lambda$ , we observe some monotonicity in the blow-up time. On the other hand, the monotonicity breaks down in the “transition” region, that is, for intermediate  $\lambda$ .

The rest of this paper is organized as follows. In Section 2, we recall some analytical results on local existence and finite time blow-up for the nonlinear Schrödinger equations that appear in this paper. For the sake of readability, proofs are given in an appendix. Numerical tests are presented in Section 3 to 5. In Section 3, we consider the dependence of the blow-up time upon  $\lambda$  in (1.1); in Section 4, we measure the dependence of the blow-up time upon a modification of the initial datum with quadratic oscillations; Section 5 is devoted to tests on (1.3) and its natural generalization in one space dimension.

## 2. SOME THEORETICAL RESULTS

In this section, we present some analytical results that provide bounds, from above and/or from below, for blow-up time. The techniques are classical: the proofs rely on Strichartz estimates, conservations of mass and energy, and pseudo-conformal conservation law. Yet, it seems that the explicit dependence of the existence time upon some parameters had not been investigated before, except in [9] (see Section 2.2). These results are somehow a more quantitative motivation for the numerical tests that follow. Technical proofs are given in Appendix A.

**2.1. Generalities.** We first state a local existence result, from which we infer a lower bound on the blow-up time. Recall that in (1.1), we consider only nonnegative time.

**Proposition 2.1.** *Let  $\lambda > 0$ ,  $\sigma \geq \frac{2}{n}$  with  $\sigma < \frac{2}{n-2}$  if  $n \geq 3$ , and  $u_0 \in H^1(\mathbb{R}^n)$ . There exists  $\varepsilon > 0$  independent of  $\lambda, \sigma$  and  $u_0$  such that if*

$$(2.1) \quad \lambda T^{\frac{2-(n-2)\sigma}{2\sigma+2}} \|u_0\|_{L^2}^{\frac{\sigma}{\sigma+1}(2-(n-2)\sigma)} \|\nabla_x u_0\|_{L^2}^{\frac{n\sigma^2}{\sigma+1}} \leq \varepsilon,$$

*then (1.1) has a unique solution  $u \in C([0, T[; H^1) \cap L^{\frac{4\sigma+4}{n\sigma}}([0, T[; L^{2\sigma+2})$ . If moreover*

$$u_0 \in \Sigma := \{f \in H^1(\mathbb{R}^n) \quad ; \quad |x|f \in L^2(\mathbb{R}^n)\},$$

*then  $u \in C([0, T[; \Sigma)$ . In addition, the following quantities are independent of time:*

$$(2.2) \quad \text{Mass: } M = \|u(t)\|_{L^2} = \text{Const} = \|u_0\|_{L^2},$$

$$(2.3) \quad \text{Energy: } E = \|\nabla_x u(t)\|_{L^2}^2 - \frac{\lambda}{\sigma+1} \|u(t)\|_{L^{2\sigma+2}}^{2\sigma+2} = \text{Const}.$$

This result is standard (see e.g. [8]), except that usually Condition (2.1) is not given explicitly: see Section A.1 for the proof. Note that in Corollary 2.2 below, we modify this condition, to a somehow weaker one. The reason is that in Proposition 2.1, local solutions are constructed without taking the conservations of mass and energy into account. We shall not recall explicitly the fact that for small initial data, the solution to (1.1) does not blow up. Indeed, for small data, the conservations of mass and energy yield an *a priori* bound on the  $H^1$ -norm of the solution, thus ruling out finite time blow-up. In our case, small initial data means that, for instance,  $\lambda^{1/(2\sigma)}\|u_0\|_{H^1} \leq \delta$  for some constant  $\delta$  depending only on  $n$  and  $\sigma$ . We shall not insist on that aspect, since our analysis is focused on regimes where blow-up does occur. This is why in the next two corollaries,  $\lambda$  is morally “large”, while  $u_0$  is fixed.

**Corollary 2.2.** *Let  $\lambda > 0$ ,  $\sigma \geq \frac{2}{n}$  with  $\sigma < \frac{2}{n-2}$  if  $n \geq 3$ , and  $u_0 \in H^1(\mathbb{R}^n)$ . There exists  $\varepsilon > 0$  independent of  $\lambda$  such that if*

$$(2.4) \quad (\lambda^{2\sigma}\|\nabla_x u_0\|_{L^2}^{4\sigma} + 1) T^{2-(n-2)\sigma} \leq \varepsilon,$$

*then (1.1) has a unique solution  $u \in C([0, T[; H^1) \cap L^{\frac{4\sigma+4}{n\sigma}}([0, T[; L^{2\sigma+2})$ . If moreover  $u_0 \in \Sigma$ , then  $u \in C([0, T[; \Sigma)$ .*

The proof of Corollary 2.2 is given in Section A.2.

**Corollary 2.3** (Dependence with respect to the coupling constant). *Let  $\lambda > 0$ ,  $\sigma \geq \frac{2}{n}$  with  $\sigma < \frac{2}{n-2}$  if  $n \geq 3$ , and  $u_0 \in \Sigma$ . Assume that  $u$  blows up in finite time  $T^* > 0$ .*

1. *We have  $T^* \geq C \langle \lambda \rangle^{-\frac{2\sigma}{2-(n-2)\sigma}}$ , for some constant  $C$  independent of  $\lambda$ , where  $\langle \lambda \rangle = \sqrt{1 + \lambda^2}$ .*
2. *If in addition  $E < 0$ , then  $T^* \leq C' \langle \lambda \rangle^{-1/2}$ , for some constant  $C'$  independent of  $\lambda$ .*

*Remark.* The above constants  $C$  and  $C'$  are independent of  $\lambda$ , but depend on the other parameters,  $u_0$ ,  $n$  and  $\sigma$ . As a matter of fact, the construction we use yields constants depending only on  $\|u_0\|_\Sigma$ ,  $n$  and  $\sigma$ .

*Proof.* The first part is a straightforward consequence of Corollary 2.2. The second follows from the Zakharov–Glassy method [32, 14]. Introduce

$$y(t) = \int_{\mathbb{R}^n} |x|^2 |u(t, x)|^2 dx.$$

Then since  $\lambda > 0$  and  $\sigma \geq \frac{2}{n}$ , we have:  $\ddot{y}(t) \leq 8n\sigma E$ , where  $E$  denotes the energy defined in Proposition 2.1. Integrating, we infer that for large  $\lambda$ ,  $y(t) \leq -C\lambda t^2$ , for some positive  $C$  independent of  $\lambda$ . Since  $y(t) \geq 0$  so long as  $u$  remains in  $\Sigma$ , this yields the second point of the corollary.  $\square$

We always have  $\frac{2\sigma}{2-(n-2)\sigma} > \frac{1}{2}$ , so the above two bounds go to zero with different rates when  $\lambda \rightarrow +\infty$ . Condition (2.1) would yield only  $T^* \geq C \langle \lambda \rangle^{-\frac{2\sigma+2}{2-(n-2)\sigma}}$ . Without even trying to see if any of these bounds is sharp, we ask the following question:

**Question 1.** *For  $\sigma \geq \frac{2}{n}$  and a fixed initial datum  $u_0 \in \Sigma$ , is the blow-up time for  $u$  solution to (1.1) monotonous with respect to  $\lambda$ ?*

This issue is addressed numerically in Section 3, where our results show that the answer to the above question should be no.

**2.2. Initial data with quadratic oscillations.** Like in [9], we now fix the equation, and alter only the initial data, with quadratic oscillations:

$$(2.5) \quad i\partial_t u + \Delta u = -|u|^{2\sigma} u, \quad x \in \mathbb{R}^n \quad ; \quad u|_{t=0} = u_0(x),$$

with  $u_0 \in \Sigma$ . For  $a \neq 0$ , define:

$$(2.6) \quad v(t, x) = \frac{e^{i\frac{|x|^2}{4(t-a)}}}{h(t)^{n/2}} u\left(\frac{at}{a-t}, \frac{x}{h(t)}\right), \quad \text{where } h(t) = \frac{a-t}{a}.$$

Then  $v$  solves:

$$(2.7) \quad i\partial_t v + \Delta v = -h(t)^{n\sigma-2} |v|^{2\sigma} v \quad ; \quad v|_{t=0} = u_0(x) e^{-i\frac{|x|^2}{4a}}.$$

In the conformally invariant case  $\sigma = 2/n$ ,  $v$  solves the same equation as  $u$ . The only difference is the presence of (additional) quadratic oscillations in the data.

**Proposition 2.4.** *Let  $u_0 \in \Sigma$  and  $2/n \leq \sigma < 2/(n-2)$ . Suppose that  $u$  blows up at time  $T > 0$ . Let  $a \in \mathbb{R}^*$ .*

- If  $a > 0$ , then  $v$  blows up at  $T_a(v) = \frac{a}{a+T} T < T$ .
- If  $a < 0$  and  $a+T < 0$ , then  $v$  blows up at  $T_a(v) = \frac{a}{a+T} T > T$ .
- If  $a < 0$  and  $a+T \geq 0$ , then  $v$  is globally defined in  $\Sigma$  for positive times (but blows up in the past if  $a+T > 0$ ).

For the critical case  $\sigma = 2/n$ , this result is proved in [9] (see also [8]). We sketch a slightly different proof in Appendix A.3, which easily includes the case  $2/n < \sigma < 2/(n-2)$ .

In the super-critical case, a natural question is to understand the role of the function  $h$ . Introduce  $w$  solving:

$$(2.8) \quad i\partial_t w + \Delta w = -|w|^{2\sigma} w \quad ; \quad w|_{t=0} = u_0(x) e^{-i\frac{|x|^2}{4a}}.$$

**Proposition 2.5.** *Let  $u_0 \in \Sigma$  and  $2/n < \sigma < 2/(n-2)$ .*

- Let  $T_a(w)$  denote the maximal existence time in the future for  $w$ . Then there exists  $C = C(\|u_0\|_\Sigma, n, \sigma)$  independent of  $a$  such that:

$$T_a(w) \geq C|a|^{\frac{4\sigma}{2-(n-2)\sigma}}.$$

- If the energy  $E$  of  $u$  is negative, then for  $a > 0$ ,  $w$  blows up at time  $T_a(w) \leq a$ .

The first point is a direct consequence of Corollary 2.2. The second point is proven in [9], and relies on the pseudo-conformal law for  $w$ .

To understand the influence of the quadratic oscillations on the blow-up time, we have to compare the blow-up time of  $u$  and that of  $w$ . In the critical case, the blow-up time depends explicitly on the magnitude of the quadratic oscillations *via* Proposition 2.4, since  $v \equiv w$  by conformal invariance. In the super-critical case, we ask:

**Question 2.** For  $\sigma > \frac{2}{n}$  and a fixed  $u_0 \in \Sigma$ , is the blow-up time for  $w$  solving (2.8) monotonous with respect to  $a$ ?

This issue is addressed numerically in Section 4: we first compare the numerics with the analytical results in the conformally invariant case, then perform tests in the supercritical case which indicate that the answer to the question above should be no.

**2.3. Damped equation.** We now consider:

$$(2.9) \quad i\partial_t \psi + \Delta \psi = -|\psi|^{2\sigma} \psi - i\delta \psi, \quad (t, x) \in \mathbb{R}_+ \times \mathbb{R}^n \quad ; \quad \psi|_{t=0} = u_0,$$

for  $\delta > 0$ . A direct application of (the proof of) Proposition 2.1 shows that  $\psi$  is defined on  $[0, T[$  for  $T \geq C|\delta|^{-1}$ . Note that the sign of  $\delta$  is irrelevant at this stage. To take damping effects into account, introduce

$$u(t, x) = e^{\delta t} \psi(t, x).$$

Then  $u$  solves:

$$(2.10) \quad i\partial_t u + \Delta u = -e^{-2\sigma\delta t} |u|^{2\sigma} u \quad ; \quad u|_{t=0} = u_0.$$

For  $\delta$  sufficiently large,  $u$  is defined globally in time, in the future:

**Proposition 2.6.** Let  $\sigma \geq \frac{2}{n}$  with  $\sigma < \frac{2}{n-2}$  if  $n \geq 3$ , and  $u_0 \in H^1(\mathbb{R}^n)$ . There exists  $C = C(\sigma, n)$  depending only on  $\sigma$  and  $n$  such that if

$$(2.11) \quad \delta^{\sigma+1} \geq C \|u_0\|_{L^2}^{\sigma(2-(n-2)\sigma)} \|\nabla u_0\|_{L^2}^{n\sigma^2},$$

then (2.10) has a unique solution  $u \in C(\mathbb{R}_+; H^1) \cap L^{\frac{4\sigma+4}{n\sigma}}(\mathbb{R}_+; L^{2\sigma+2})$ .

The proof is given in Section A.4. The following question is addressed numerically in Section 5:

**Question 3.** For  $\sigma \geq \frac{2}{n}$  and a fixed  $u_0 \in \Sigma$ , is the blow-up time for  $u$  solution to (2.10) monotonous with respect to  $\delta > 0$ ?

The simulations show that the answer is no.

### 3. NUMERICAL TEST, DEPENDENCE ON $\lambda$

We perform numerical tests by using a direct discretization method for equation (1.1), respectively (2.10). By this approach no restrictions are imposed on simulations on the closeness to eventual blow-up points in space and time and by the evolution in places “not close” to the blow-up. We employ two different numerical methods: the Time-Splitting Spectral method (TSSP), and the Relaxation method (RS).

The TSSP is based on an operator splitting method, the split-step method. The split-step method is based on a decomposition of the flow of the nonlinear equation (1.1) (or (2.10)). Define the flow  $X^t$  as the flow of the linear Schrödinger equation

$$\begin{cases} i\partial_t v + \Delta v = 0, & x \in \mathbb{R}^n, t > 0, \\ v(x, 0) = v_0(x), & x \in \mathbb{R}^2, \end{cases}$$

and  $Y^t$  as the flow of the nonlinear differential equation

$$\begin{cases} i\partial_t w = -g(t)|w|^{2\sigma} w, & x \in \mathbb{R}^n, t > 0, \\ w(x, 0) = w_0(x), & x \in \mathbb{R}^2. \end{cases}$$

where  $g(t) = \lambda$  for the case of (1.1) and  $g(t) = e^{-2\sigma\delta t}$  for (2.10). Then the split-step method consists of approximating the exact  $u(x, t)$  at each time step by combining the two flows  $X^t$  and  $Y^t$ . We employ here the Strang formula  $Z_S^t = X^{t/2} Y^t X^{t/2}$ , which is of second order. Higher order splitting is also possible. For a general nonlinear Schrödinger equation, a convergence proof of the splitting method was done by Besse *et al.* in [4]. For the TSSP, a spectral method is employed to compute the flow  $X^t$  of the free Schrödinger equation. The flow  $Y^t$ , which is the flow of a nonlinear ODE, can be computed exactly, since it leaves  $|w|^2$  invariant. So its integration is straightforward. The TSSP has proved to be an efficient and reliable method for NLS type equations. See for example [1, 2] for a study of the NLS in the semi-classical limit case, and [25, 5] for a more general numerical study.

For the 2-d calculations, a parallel version of the TSSP scheme is used on the parallel cluster machine “Schrödinger III” at the University of Vienna.

The Relaxation method (RS) is a discretization of finite difference type [3]. It is based on central-difference approximation shifted by a half time-step. To formulate the scheme, we rewrite the NLS equation as a system:

$$\begin{cases} i\partial_t u + \Delta u &= -g(t) \psi u, \\ \psi &= |u|^{2\sigma} \end{cases}$$

where  $g(t)$  is as above. Then the first equation is discretized by central difference quotient at the time  $t_{n+1/2} = (n + \frac{1}{2})\Delta t$ , and the second by central time average at the time  $t_n = n\Delta t$ . Let  $u^n$  be the approximation at  $t = t_n$ , then the scheme is given by

$$\begin{aligned} i \frac{u^{n+1} - u^n}{\Delta t} + \Delta_D \left( \frac{u^{n+1} + u^n}{2} \right) &= -g(t) \psi^{n+1/2} \left( \frac{u^{n+1} + u^n}{2} \right), \\ \frac{\psi^{n+1/2} + \psi^{n-1/2}}{2} &= |u^n|^{2\sigma} \end{aligned}$$

where  $\Delta_D$  denotes a finite difference Laplacian. It requires only explicit evaluations of the nonlinear term. It also conserves energy ([3]).

To determine whether blow-up is occurring or not, we calculate the two terms in the energy (2.3), kinetic and potential energy, and look for an increase of at least four orders of magnitude in both of them. The first time at which this is occurring is assumed to be the blow-up time. The space and time resolution are chosen sufficiently fine such that this increase is realized.

**3.1. Critical power.** First we consider (1.1) for  $\sigma = \frac{2}{n}$ , that is the critical case. We study the dependence of the blow-up time on the constant  $\lambda$  for a series of different data.

### Tests in one space dimension

**Test 1.** For the case  $n = 1$ , the first kind of data we study is

$$(3.1) \quad u_0(x) = C e^{-x^2} e^{-i \log(e^x + e^{-x})}.$$

The constant  $C$  is equal to 1.75 which leads to  $\|u_0\|_{L^2}^2 = 3.839$ . We take  $Np = 2^{12} = 4096$  mesh points, and several time steps according to the necessary resolution for the blow-up, with  $\Delta t = 2.5 \cdot 10^{-6}$  as smallest. The discretization domain is  $[-8, 8]$ . Figure 1 shows the blow-up time in relation to a changing  $\lambda$ . It can be observed that the blow-up time is decreasing

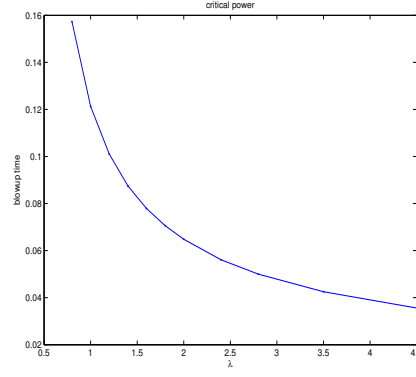


FIGURE 1. Blow-up time with varying  $\lambda$ , single Gaussian data (Test 1).

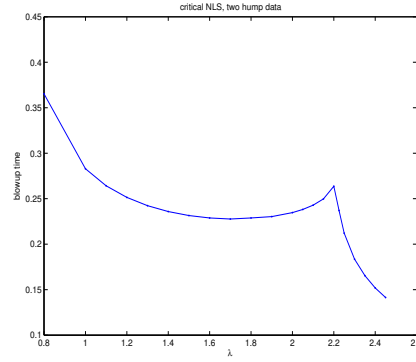


FIGURE 2. Blow-up time with varying  $\lambda$  (Test 2).

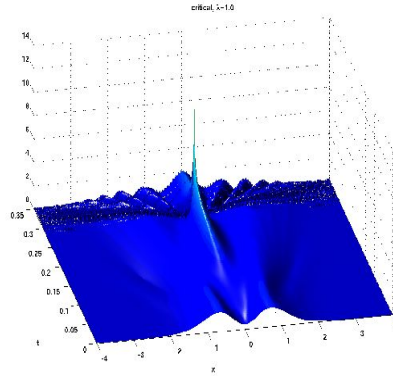


FIGURE 3. Time evolution with low potential energy.

monotonously with  $\lambda$ , as predicted by the heuristics for the case of a single Gaussian profile.

**Test 2.** The next kind of data we study is

$$(3.2) \quad u_0(x) = C \left( e^{-x^2} - 0.9e^{-3x^2} \right) e^{-i \log(e^x + e^{-x})}.$$



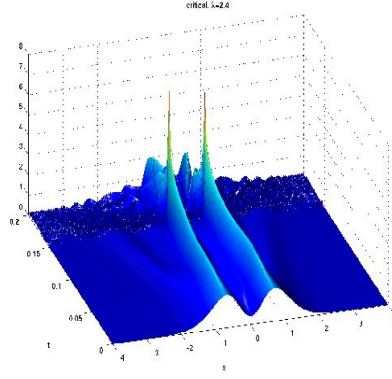


FIGURE 4. Time evolution with high potential energy.

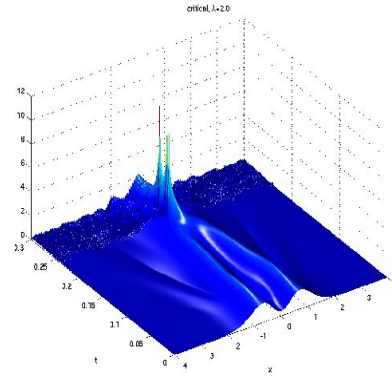


FIGURE 5. Time evolution in intermediate regime: non-monotonicity.

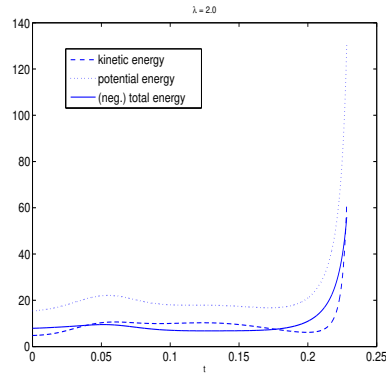


FIGURE 6. Determining blow-up time by increase of energy: (minus) total energy in comparison with kinetic and potential energy away from the blow-up

The constant  $C$  is equal to 4 which leads to  $\|u_0\|_{L^2}^2 = 3.907$ . The difference of two Gaussian profiles results in two local maxima in the modulus of  $u_0$ . The phase term has a focusing effect and its focus point does not agree with

the local maxima of the modulus. The finest discretization parameters used are  $Np = 2^{14} = 16384$ ,  $\Delta t = 2.5 \cdot 10^{-6}$ . The discretization domain is  $[-8, 8]$ .

Figure 2 shows the blow-up time in relation to a changing  $\lambda$ . It can be observed that for low and very high strengths of the nonlinearity  $\lambda$  ( $\lambda < 1.6$  and  $\lambda > 2.2$ ), the blow-up time is monotonously decreasing with  $\lambda$ , while in between there is a region where monotonicity does not hold.

Heuristically, two effects play a role in the solution with this data: the nonlinear self-focusing, which tries to focus the mass to points where the most mass is already present, and the (linear) phase influence, which tends to focus the mass at zero.

In Figures 3, 4 and 5, the time evolution of the modulus of  $u(t, x)$  is shown for values of  $\lambda$  from the three different regions of the above curve.

- Figure 3 shows the case  $\lambda = 1$ . The two initial humps merge to one hump before the blow-up, which happens at a single point. The phase focusing happens at a faster time scale than the nonlinear focusing.
- Figure 4 shows the case  $\lambda = 2.4$ . Blow-up is occurring simultaneously at two points and there are always two humps present. Apparently the nonlinear self-focusing here happens faster than phase focusing.
- Figure 5 is for  $\lambda = 2.0$ , which is in the non-monotonicity region. Blow-up here occurs at a single point, and the merging of the two humps is closer to the blow-up than in Figure 3. In this case it is not clear which of the two effects would happen at a faster time scale, nor how they would interact. Blow-up is occurring, but the blow-up time is no longer monotonous with respect to the size of the nonlinear term.

In Figure 6, we show the energy components for the case  $\lambda = 2.0$  which are used to determine the blow-up time. The kinetic energy increases by a factor of  $10^4$ , or slightly more, at the blow-up time. Figure 6 compares the kinetic and potential energy parts with  $-E(u(t))$  away from the blow-up. The TSSP scheme used for this simulation does not conserve energy. Near the blow-up time, the energy conservation is no longer true for the numerical result. Note that, outside of a time interval close to blow-up, the kinetic energy is not monotonously increasing in time.

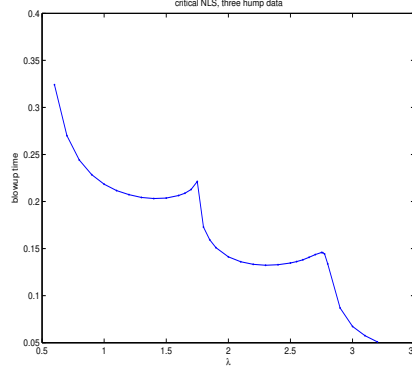
*Remark.* If the data (3.2) are used without the phase term, which leaves just a “two-hump” profile, non-monotonicity can be observed in the same way as described above. However overall blow-up times increase. Apparently the merging of the two humps can occur even without the influence of an initial phase term thanks to the mass dispersion tendency of the free evolution together with the focusing effect of the nonlinearity.

### Test 3. Data with three humps

The next test uses a sum of three Gaussians and the same phase term as before, so there are three local modulus maxima instead of two.

$$u_0(x) = C \left( e^{-(3x)^2} + e^{-(3(x-1))^2} + e^{-(3(x+1))^2} \right) e^{-i \log(e^x + e^{-x})},$$

with  $C = 2$ ,  $\|u_0\|_{L^2}^2 = 5.09$ . The discretization parameters are  $Np = 2^{12}$  mesh points and  $\Delta t = 1.5 \cdot 10^{-5}$ . The discretization domain is  $[-8, 8]$ . The blow-up times with respect to changing  $\lambda$  are shown in Figure 7. The same effect as above can be observed.

FIGURE 7. Blow-up time with varying  $\lambda$ , three hump data (Test 3).

There are two regimes for the nonlinearity strength  $\lambda$  where the blow-up time is non-monotonous. Blow-up happens either at three points, two or one point depending on  $\lambda$ .

**Test 4.** Data with two humps up, one down

In this test the data are taken to be

$$u_0(x) = C \left( e^{-(3(x-1))^2} - e^{-(3x)^2} + e^{-(3(x+1))^2} \right) e^{-i \log(e^x + e^{-x})},$$

with  $C = 2$ ,  $\|u_0\|_{L^2}^2 = 4.93$ . One of the three Gaussians has an opposite sign, so there is a constant phase shift in part of the data. The blow-up times are shown in Figure 8.

For  $\lambda < 1.6$ , there is no blow-up occurring. For larger  $\lambda$ , non-monotonicity similar to the situation above can be observed. Observe that the slope of the curve is rather steep, for  $2.7 < \lambda < 2.8$ . This shows a highly nonlinear phenomenon. Note however that there is one point on the steep line after the local maximum:

$\lambda$	$T^*$
2.7	0.1912
2.725	0.2152
2.75	0.1612
2.8	0.0555

**Test 5.** Data with one hump up, one down

We use

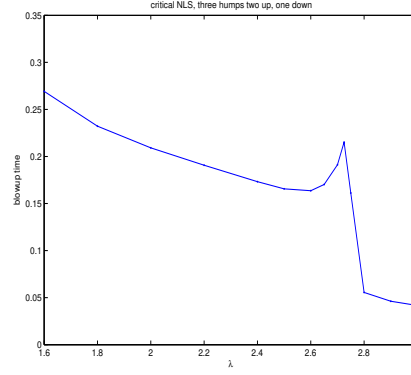
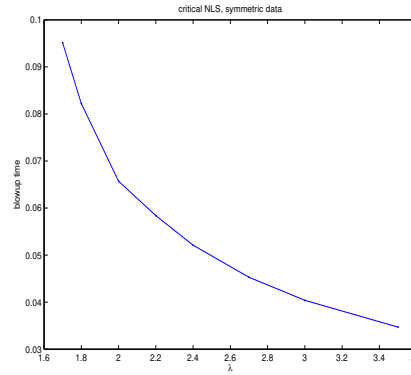
$$u_0(x) = C e^{-x^2} \tanh x e^{-i \log(e^x + e^{-x})}.$$

We use  $C = 3.0$  and  $\|u_0\|_{L^2}^2 = 4.4476$ , and discretizations of  $Np = 2^{13}$  mesh points and  $\Delta t = 2.0 \cdot 10^{-6}$ . The result is shown in Figure 9. In this case, the blow-up time is monotonous with  $\lambda$ .

*Remark.* For other point-symmetric data with more than two humps, there is monotonicity.

**Test 6.** Stability issues: asymmetric data

In order to investigate the dependence of the qualitative findings on the

FIGURE 8. Blow-up time with varying  $\lambda$ , three hump data (Test 4).FIGURE 9. Blow-up time with varying  $\lambda$ , data with point symmetry (Test 5).

symmetry of the data, we choose some data which perturb the symmetry of (3.2). We used

$$u_0(x) = C \left( e^{-x^2} - 0.9e^{-3x^2} \right) e^{-i \log 2 \cosh(x-0.25)},$$

and

$$u_0(x) = C \left( e^{-(x-1.5)^2} + 0.99e^{-(x+1.5)^2} \right) e^{-i \log(e^x + e^{-x})},$$

to have either a phase that focuses away from the symmetry point between the two humps, or two humps of different heights. It turns out that non-monotonicity can be observed for both of these cases, too. The perturbations to (3.2) tested here are small enough not to hinder non-monotonous blow-up times.

### Test in two space dimensions

**Test 7.** For the test in two space dimensions, we extend (3.2) by making the phase term radially symmetric and multiplying the one-dimensional two-hump profile by a single Gaussian in the second space dimension:

$$(3.3) \quad u_0(x, y) = C \left( e^{-x^2} - 0.9e^{-3x^2} \right) e^{-y^2} e^{-i \log 2 \cosh(\sqrt{x^2 + y^2})}.$$

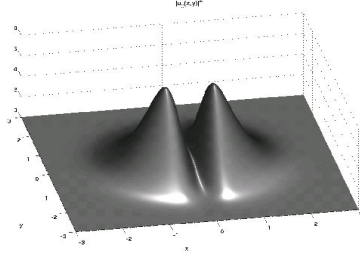


FIGURE 10. Initial data for two dimensional case, modulus (Test 7).

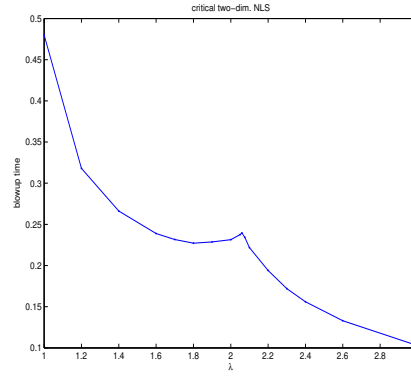
FIGURE 11. Blow-up time with varying  $\lambda$ , two dimensional case (Test 7).

Figure 10 shows the modulus of (3.3). We choose  $C = 7.0$ ,  $\|u\|_{L^2}^2 = 15.0$ . The smallest discretization parameters used are  $Np = 2^{12}$  mesh points and  $\Delta t = 1 \cdot 10^{-5}$  with the discretization domain  $[-4, 4]^2$ .

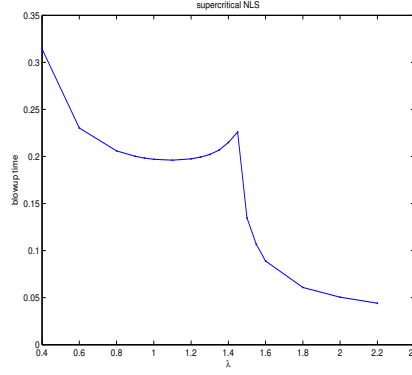
The blow-up times with changing  $\lambda$  are shown in Figure 11. Non-monotonicity can be observed.

### 3.2. Supercritical power.

**Test 8.** We tested equation (1.1) in one space dimension, with  $\sigma = 3$  and the data (3.2) ( $C = 3.5$ , hence  $\|u_0\|_{L^2}^2 = 2.99$ ). The discretization parameters are  $\Delta x = 0.0039$ , and up to  $\Delta t = 1 \cdot 10^{-6}$ . The discretization domain is  $[-8, 8]$ . The blow-up time with varying  $\lambda$  is shown in Figure 12. Also in the supercritical case, non-monotonicity of blow-up times can be observed.

## 4. NUMERICAL TEST, DEPENDENCE ON QUADRATIC OSCILLATIONS

We turn to equation (2.7) and investigate the dependence of blow-up time on the scale of quadratic oscillations. To compare the simulations to the result of Proposition 2.4, we simulate (2.5) with the same data to obtain

FIGURE 12. Blow-up time with varying constant  $\lambda$  (Test 8).

the blow-up time for this equation, and then plot the curve of  $T_a$  that is predicted in Proposition 2.4 for the two regions  $a > 0$  and  $a < 0$ ,  $a + T < 0$ .

**4.1. Critical power.** We use (2.7) in space dimension one, with  $\sigma = 2$  with various  $u_0(x)$ .

**Test 9.** Single hump: We take

$$u_0(x) = C e^{-x^2}$$

with  $C = 1.75$ . The discretization parameters in this and the two following tests are  $Np = 2^{14}$  mesh points and  $\Delta t = 4 \cdot 10^{-6}$ . The discretization domain is  $[-8, 8]$  for all cases except the two largest negative  $a$  in Test 9 and 10. Here the domain is extended to  $[-18, 18]$  and the space resolution is  $Np = 2^{13}$  resp.  $[-40, 40]$  and  $Np = 2^{14}$  for the largest negative  $a$  of Test 11. Figure 13 shows the blow-up time of  $v$  in relation to the scale  $a$  of quadratic oscillations in the data. We use both positive  $a$  and negative  $a$  with  $a + T < 0$ . Asterisks denote the blow-up times and the dashed line shows the result of Proposition 2.4 with  $T$  obtained by a simulation of (2.5). It can be observed that the results agree very well. In each of the two regions for  $a$  that have been used in this test, the blow-up time is monotonous with respect to  $a$ .

**Test 10.** Two humps: We take

$$u_0(x) = C \left( e^{-x^2} - 0.9e^{-3x^2} \right)$$

which is the same as (3.2) without the phase term that appears there. We take  $C = 4.0$ . Figure 14 shows the blow-up times marked by asterisks. As above the dashed line shows the modified blow-up time according to Proposition 2.4. The two curves agree.

**Test 11.** Two humps with additional phase: Here we use

$$u_0(x) = C \left( e^{-x^2} - 0.9e^{-3x^2} \right) e^{-i \log(e^x + e^{-x})}$$

which is the same as (3.2). Figure 15 shows the blow-up times of the simulations and according to the Proposition as above. The results agree.

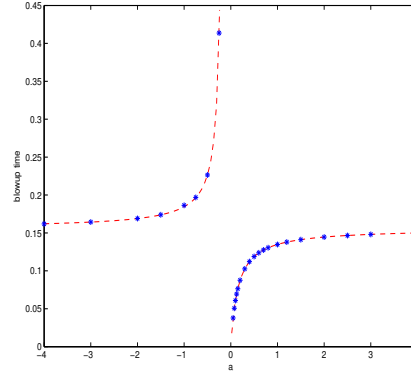


FIGURE 13. Blow-up time with varying  $a$  in quadratic oscillations, critical power (Test 9).

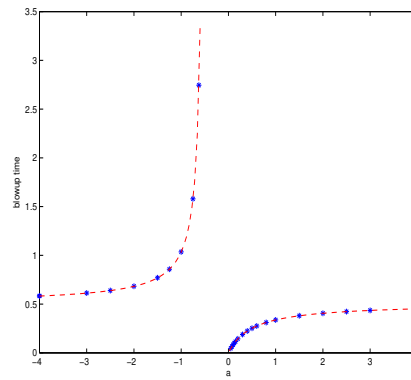


FIGURE 14. Blow-up time with varying  $a$  in quadratic oscillations, critical power, two hump data (Test 10).

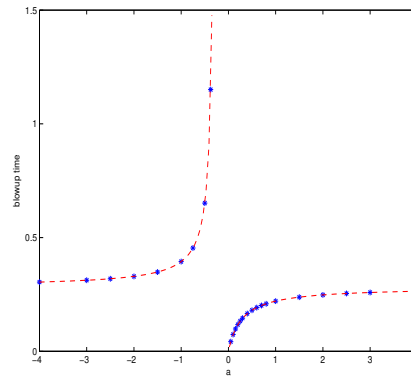


FIGURE 15. Blow-up time with varying  $a$  in quadratic oscillations, critical power, data with additional phase (Test 11).

**4.2. Supercritical power.** We now consider Eqns. (2.7) and (2.8) with  $\sigma = 3$ , in space dimension one. We give results for both  $w$  and  $v$ . We use the same series of data as for the critical power case.

The discretization parameters in Tests 12 to 14 are  $Np = 2^{13}$  mesh points and  $\Delta t = 1 \cdot 10^{-5}$ , down to  $\Delta t = 4 \cdot 10^{-6}$ .

**Test 12.** Single hump: We take  $u_0(x) = C e^{-x^2}$ . Figure 16 shows the blow-up time in relation to the scale  $a$  of quadratic oscillations in the data. In the left figure, the dashed line is the calculated blow-up time for  $v$  and the asterisks mark the simulated blow-up times. The right figure compares the blow-up times for  $v$  and  $w$ , where  $w$  is denoted by asterisks and  $v$  by dots joined by a line. We can see that  $w$  blows up a bit earlier than  $v$  for positive  $a$ . For negative  $a$ , it blows up a bit later, but the blow-up times are rather close to those of  $v$  as in the positive  $a$  case. Again the blow-up times for  $v$  match the result of Proposition 2.4.

**Test 13.** Two humps: We take  $u_0(x) = C \left( e^{-x^2} - 0.9e^{-3x^2} \right)$ . Figure 17 shows the blow-up time of  $v$  in relation to  $a$ .

**Test 14.** Two humps with additional phase: Here we use

$$u_0(x) = C \left( e^{-x^2} - 0.9e^{-3x^2} \right) e^{-i \log(e^x + e^{-x})}.$$

Figure 18 shows the blow-up time of  $v$  in relation to  $a$ .

**Test 15.** Two humps placed asymmetrically: Here we use

$$u_0(x) = C \left( e^{-(3x)^2} + e^{-(3(x-1.5))^2} \right).$$

We take  $C = 1.8$ . The smallest discretization parameters used in this test are  $Np = 2^{15}$  mesh points and  $\Delta t = 1.5 \cdot 10^{-6}$ . The computation domain is  $[-8, 8]$ , except for the largest value of  $a$ . Figure 19 shows the blow-up time for  $w$  in relation to  $a$  obtained by the two numerical methods employed: the circles represent simulations done by the TSSP, the asterisks simulations by the RS. In addition a solid line displays the blow-up times for  $v$ . Non-monotonicity can be observed, which answers question 2 in a negative way. The blow-up time of  $w$  is always smaller than that of  $v$ . We also see that the results of the two different schemes agree in a good way. Note that the occurrence of non-monotonicity is very sensitive to the size of the data. If we choose  $C = 1.7$  or  $1.9$  instead of  $C = 1.8$ , monotonicity can be observed.

*Remark 4.1* (Test 15). Leave out the question of quadratic oscillations, and consider  $u$  solving (2.5). Its blow-up time as a function of the constant  $C$  is given by:

$C$	$T^*$
1.795	0.528
1.798	0.480
1.8	0.462
1.804	0.446
1.808	0.507
1.81	0.076
1.82	0.048

Since changing  $C$  in (2.5) is equivalent to changing  $\lambda$  in (1.1), we see here a behavior analogous to Test 8 (Figure 12), where similar data are used. The value  $C = 1.8$  is very close to (actually slightly below) the potential energy level where the blow-up changes from two point blow-up to one point blow-up, and non-monotonicity can be observed.



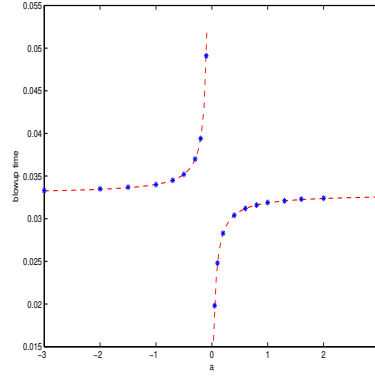


FIGURE 16. Blow-up time with varying  $a$  in quadratic oscillations, supercritical power. Left: blow-up times for  $v$ . Right: comparison of  $v$  and  $w$ , dots with line for  $v$ , asterisks for  $w$  (Test 12).

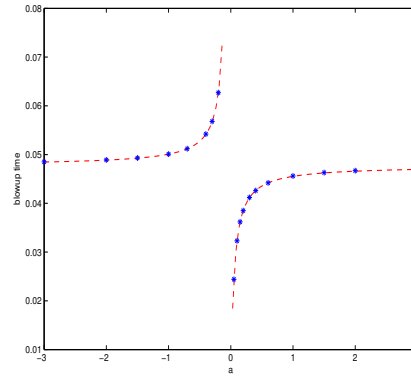


FIGURE 17. Blow-up time of  $v$  with varying  $a$  in quadratic oscillations, supercritical power (Test 13).

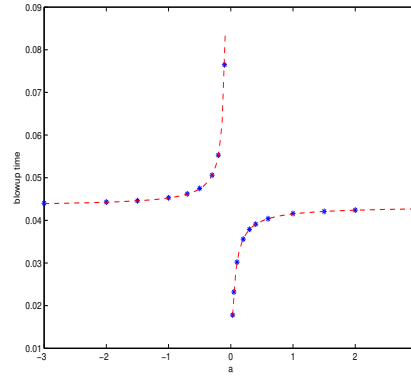


FIGURE 18. Blow-up time of  $v$  with varying  $a$  in quadratic oscillations, supercritical power, data with additional phase (Test 14).

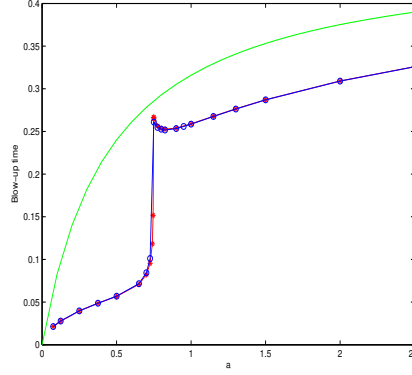


FIGURE 19. Blow-up time for  $w$  with varying  $a$  in quadratic oscillations, supercritical power, asymmetric data (asterisks and circles). Solid line: Blow-up time for  $v$ . (Test 15).

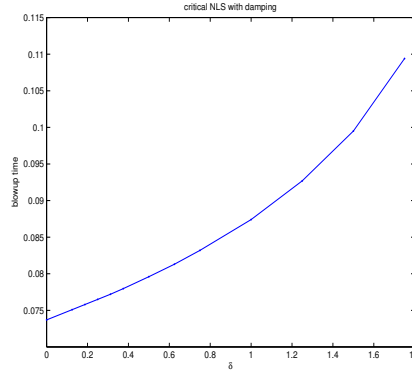


FIGURE 20. Blow-up time with varying damping constant  $\delta$  (Test 16).

## 5. NUMERICAL TEST, DAMPED NLS

**5.1. Critical power.** We now turn to (2.10).

### Test in one space dimension

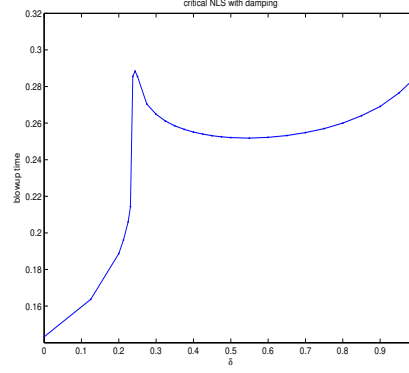
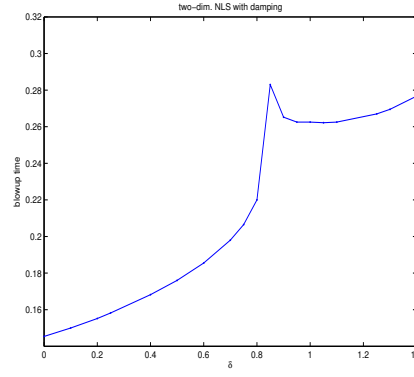
**Test 16.** For (2.10) in space dimension one, we first use the single Gaussian data (3.1). The scale  $C = 2$  was chosen so that  $\|u_0\|_{L^2}^2 = 5.013$ , the smallest discretization parameters used are  $Np = 2^{12}$  mesh points and  $\Delta t = 2.5 \cdot 10^{-6}$ . The blow-up time with respect to changing  $\delta$  is shown in Figure 20. The blow-up time is decreasing monotonically with  $\delta$ , in accordance with the arguments of [11]. For  $\delta > 1.75$ , blow-up is prevented.

**Test 17.** Next we use the “two-hump” data (3.2). The data scale was chosen as  $C = 5$  so that  $\|u_0\|_{L^2}^2 = 11.969$ .

The finest discretization parameters used in this test are  $Np = 2^{14}$  mesh-points and  $\Delta t = 2.5 \cdot 10^{-7}$ .

The blow-up time with respect to changing  $\delta$  is shown in Figure 21. It can be seen that the blow-up time is not monotonously increasing with  $\delta$ . The effect is somehow more pronounced than in the case of Equation (1.1).

### Test in two space dimensions

FIGURE 21. Blow-up time with varying damping constant  $\delta$  (Test 17).FIGURE 22. Blow-up time with varying damping constant  $\delta$  (Test 18).

**Test 18.** For the two-dimensional case of (2.10), we use the data (3.3) with  $C = 11$ , so that the initial mass is  $\|u_0\|_{L^2}^2 = 37.04$ . This is above the minimal value necessary for blow-up ([11]). The finest discretization parameters used in this test are  $Np = 2^{11}$  meshpoints and  $\Delta t = 5.0 \cdot 10^{-6}$ . The discretization domain is  $[-8, 8]^2$ .

The blow-up time in dependence of  $\delta$  is shown in Figure 22. For  $\delta > 1.4$ , blow-up is prevented.

## 5.2. Supercritical Power.

**Test 19.** We tested equation (2.10) in space dimension one with  $\sigma = 3$ . The data are chosen as (3.2) with  $C = 3.8$ , so  $\|u_0\|_{L^2}^2 = 3.53$ . The discretization parameters used in this test are  $Np = 2^{12}$  meshpoints and  $\Delta t = 5.0 \cdot 10^{-6}$  or  $\Delta t = 10^{-5}$ . The discretization domain is  $[-8, 8]$ .

The blow-up times with respect to the damping constant  $\delta$  are shown in Figure 23. Also in this case monotonicity is not true. For  $\delta > 1.17$ , blow-up is prevented. In this case, the occurrence of non-monotonicity is very sensitive to the size of the data, as already observed in Test 16. If we choose  $C = 3.6$  or  $4.0$ , instead of  $C = 3.8$ , we observe monotonicity.

**Test 20.** We repeat Test 19 with a different scale of the data, we take  $C = 3.6$  in (3.2), so that  $\|u_0\|_{L^2}^2 = 3.17$ . The discretization parameters used

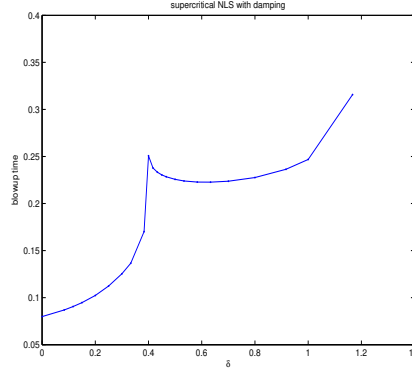


FIGURE 23. Blow-up time with varying damping constant  $\delta$ , supercritical power (Test 19).

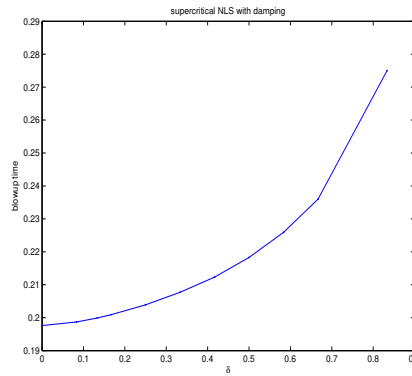


FIGURE 24. Blow-up time with varying damping constant  $\delta$ , supercritical power (Test 20).

in this test are  $Np = 2^{15}$  mesh points and  $\Delta t = 5.0 \cdot 10^{-6}$ . The discretization domain is  $[-8, 8]$ . The blow-up times with respect to the damping constant  $\delta$  are shown in Figure 24. We can see that the blow-up is monotonous in  $\delta$ . The blow-up always happens a single point at the origin, and for  $\delta > 0.83$ , blow-up is prevented.

All tests were done with both the TSSP and the Relaxation scheme (RS). The results agree, as an example we showed the comparison of the schemes in figure 19. By using two numerical schemes with different discretization approaches, the possibility of observing just numerical defects introduced by a particular discretization method can be excluded. The effects of non-monotonicity found here can be seen with two inherently different numerical methods, which is an indication that the observations are not related to numerical errors but indeed analytical properties.

## 6. CONCLUSION

In this paper, we have addressed numerically the question of the dependence of the blow-up time for solutions to nonlinear Schrödinger equations upon one specific parameter, in three cases:

- Dependence upon the coupling constant  $\lambda$ , for fixed  $n, \sigma$  and  $u_0$ :

$$i\partial_t u + \Delta u = -\lambda|u|^{2\sigma}u, \quad (t, x) \in \mathbb{R}_+ \times \mathbb{R}^n \quad ; \quad u|_{t=0} = u_0.$$

- Dependence upon the magnitude of a quadratic oscillation introduced in the initial data: only  $a$  varies in the following equation,

$$i\partial_t w + \Delta w = -|w|^{2\sigma}w \quad ; \quad w|_{t=0} = u_0(x)e^{-i\frac{|x|^2}{4a}}.$$

- Dependence upon the strength of the damping  $\delta \geq 0$  in

$$i\partial_t \psi + \Delta \psi = -|\psi|^{2\sigma}\psi - i\delta\psi \quad ; \quad \psi|_{t=0} = u_0.$$

In the  $L^2$  super-critical case  $\sigma > \frac{2}{n}$ , the tests we performed highly suggest that in either of the above three cases, the blow-up time is not monotonous with respect to the variation of the parameter considered.

In the  $L^2$  critical case  $\sigma = \frac{2}{n}$ , there is apparently no monotonicity in the first and in the third problem. In the second one however, our tests agree with the analytical result: there is monotonicity of the blow-up time with respect to  $a$ , as recalled in Proposition 2.4.

We used two numerical methods (time-splitting spectral method and a relaxation method), for the results observed to be more convincing. We may say that they are, since the two methods yield the same results (and not only just similar results, see Figure 19).

Note that in some cases where we observed monotonicity reversal, the slope of the blow-up time/varying parameter curve may be rather steep near the monotonicity breakup. Compare Figure 8 near  $\lambda = 2.7$  with Figure 1. In the quadratic oscillations case, Figure 19 shows a similar feature near  $a = 0.7$ . For the equation with a damping term, compare Figures 21 and 22 with Figure 20. This suggests that the underlying mechanism causing the monotonicity reversal is strongly nonlinear. It seems inappropriate to speak of instability though (for instance in Figure 8, we saw that there is one point on the steep line after the local maximum). In these examples, the blow-up time changes rather fast compared to the modification of the  $L^2$ -norm of the initial data (see also Remark 4.1). Yet, the dependence of the blow-up time might also involve other analytical quantities, or geometrical features.

All the numerical counter-examples to monotonicity that we found contain a somehow nontrivial profile, inasmuch as the initial datum is formed of two (or more) humps. The question of an analytical justification remains open and challenging in these cases.

## APPENDIX A. PROOFS

**A.1. Proof of Proposition 2.1.** It is based on a fixed point argument using Strichartz estimates, which we first recall.

**Definition A.1.** A pair  $(q, r)$  is **admissible** if  $2 \leq r \leq \frac{2n}{n-2}$  (resp.  $2 \leq r \leq \infty$  if  $n = 1$ ,  $2 \leq r < \infty$  if  $n = 2$ ) and

$$\frac{2}{q} = \delta(r) := n \left( \frac{1}{2} - \frac{1}{r} \right).$$

**Lemma A.1** (Strichartz estimates, see e.g. [31, 13, 16]). *Let  $(q, r)$ ,  $(q_1, r_1)$  and  $(q_2, r_2)$  be admissible pairs. Denote  $U(t) := e^{it\Delta}$ .*

1. *There exists  $C_r$  such that for any  $\varphi \in L^2(\mathbb{R}^n)$ :*

$$(A.1) \quad \|U(\cdot)\varphi\|_{L^q(\mathbb{R}; L^r)} \leq C_r \|\varphi\|_{L^2}.$$

2. *There exists  $C_{r_1, r_2}$  such that for any interval  $I$  and any  $F \in L^{q'_2}(I; L^{r'_2})$ :*

$$(A.2) \quad \left\| \int_{I \cap \{s \leq t\}} U(t-s) F(s) ds \right\|_{L^{q_1}(I; L^{r_1})} \leq C_{r_1, r_2} \|F\|_{L^{q'_2}(I; L^{r'_2})}.$$

The proof of Proposition 2.1 relies on the following straightforward lemma:

**Lemma A.2.** *Let  $r = s = 2\sigma + 2$ , and  $q = \frac{4\sigma+4}{n\sigma}$ , so that the pair  $(q, r)$  is admissible. Define  $k$  by*

$$k = \frac{2\sigma(2\sigma + 2)}{2 - (n-2)\sigma}.$$

*Then  $k$  is finite, and the following algebraic identities hold:*

$$\frac{1}{r'} = \frac{1}{r} + \frac{2\sigma}{s} \quad ; \quad \frac{1}{q'} = \frac{1}{q} + \frac{2\sigma}{k}.$$

*Proof of Proposition 2.1.* For  $A \in \{\text{Id}, \nabla_x\}$ , denote  $R_A := \|Au_0\|_{L^2}$ . With the notations of Lemmas A.1 and A.2, define:

$$X_T := \{u \in C([0, T]; H^1) ; Au \in L^\infty([0, T]; L^2) \cap L^q([0, T]; L^r), \\ \|Au\|_{L^\infty([0, T]; L^2)} \leq 2R_A, \|Au\|_{L^q([0, T]; L^r)} \leq 2C_{2\sigma} R_A, \forall A \in \{\text{Id}, \nabla_x\}\}.$$

Duhamel's formula for (1.1) writes:

$$(A.3) \quad u(t) = U(t)u_0 + i\lambda \int_0^t U(t-s) (|u|^{2\sigma} u)(s) ds.$$

Denote  $F(u)$  the right hand side of (A.3). We prove that  $F$  maps  $X_T$  into itself and is a contraction (in a weaker metric) provided that (2.1) is satisfied, for  $\varepsilon > 0$  sufficiently small. Denote  $L_T^a := L^a([0, T])$ . From Lemmas A.1 and A.2, we have, for  $A \in \{\text{Id}, \nabla_x\}$ :

$$(A.4) \quad \|A(F(u))\|_{L_T^\infty(L^2)} \leq \|Au_0\|_{L^2} + C\lambda \|A(|u|^{2\sigma} u)\|_{L_T^{q'}(L^{r'})} \\ \leq \|Au_0\|_{L^2} + C\lambda \|u\|_{L_T^k(L^s)}^{2\sigma} \|Au\|_{L_T^q(L^r)},$$

for some constant  $C$  depending only on  $n$  and  $\sigma$ . From Gagliardo–Nirenberg inequality, we have:

$$\|u(t)\|_{L^s} \leq C(n, s) \|u(t)\|_{L^2}^{1-\delta(s)} \|\nabla_x u(t)\|_{L^2}^{\delta(s)},$$

where  $\delta(s)$  is given in Definition A.1. We infer, for  $u \in X_T$ :

$$\|A(F(u))\|_{L_T^\infty(L^2)} \leq R_A + C\lambda T^{2\sigma/k} R_{\text{Id}}^{2\sigma(1-\delta(s))} R_{\nabla_x}^{2\sigma\delta(s)} R_A,$$

where from now on, we denote by  $C$  all the constants which do not depend on relevant parameters. Using Lemma A.1, we have similarly:

$$\|A(F(u))\|_{L_T^q(L^r)} \leq C_r R_A + C\lambda T^{2\sigma/k} R_{\text{Id}}^{2\sigma(1-\delta(s))} R_{\nabla_x}^{2\sigma\delta(s)} R_A,$$

for some other constant  $C$  depending only on  $n$  and  $\sigma$ . We therefore have stability for

$$(A.5) \quad \lambda T^{2\sigma/k} R_{\text{Id}}^{2\sigma(1-\delta(s))} R_{\nabla_x}^{2\sigma\delta(s)} \ll 1.$$

We have contraction in the weaker metric  $L^q([0, T]; L^r)$  under a similar condition:

$$\begin{aligned} \|F(u_2) - F(u_1)\|_{L_T^q(L^r)} &\leq C_{r,r} \lambda \left\| (|u_2|^{2\sigma} u_2 - |u_1|^{2\sigma} u_1) \right\|_{L_T^{q'}(L^{r'})} \\ &\leq C \lambda \left( \|u_1\|_{L_T^k(L^s)}^{2\sigma} + \|u_2\|_{L_T^k(L^s)}^{2\sigma} \right) \|u_2 - u_1\|_{L_T^q(L^r)} \\ &\leq C \lambda T^{2\sigma/k} R_{\text{Id}}^{2\sigma(1-\delta(s))} R_{\nabla_x}^{2\sigma\delta(s)} \|u_2 - u_1\|_{L_T^q(L^r)}. \end{aligned}$$

If (A.5) is satisfied, then  $F$  has a unique fixed point in  $X_T$ . Since (A.5) is nothing else but (2.1), this proves the first part of Proposition 2.1.

When  $u_0 \in \Sigma$ , one can prove that the  $\Sigma$ -regularity is conserved along the time evolution by now considering  $A \in \{\text{Id}, \nabla_x, J(t)\}$ , where  $J(t) = x + 2it\nabla_x$  is the Galilean operator. (This operator commutes with the group  $U(t)$  and acts on the nonlinearity we consider like a derivative.) Finally, we refer to [8] for the conservation laws.  $\square$

**A.2. Proof of Corollary 2.2.** In the above proof of local existence, we did not use the conservation laws. We now take them into account.

Consider Duhamel's formula (A.3), and seek an  $L_t^\infty(L_x^2)$ -bound for  $\nabla_x u$ . For  $A \in \{\text{Id}, \nabla_x\}$ , we have like above:

$$\|Au\|_{L_T^q(L^r)} \leq C_r \|Au_0\|_{L^2} + C \lambda \|u\|_{L_T^k(L^s)}^{2\sigma} \|Au\|_{L_T^q(L^r)}.$$

Recall that  $s = 2\sigma + 2$ ; from the conservation of energy,

$$\|u(t)\|_{L^s} \leq C \lambda^{-1/s} \left( \|\nabla_x u(t)\|_{L^2}^{2/s} + |E| \right) \leq C \left( \lambda^{-1/s} \|\nabla_x u(t)\|_{L^2}^{2/s} + 1 \right),$$

for  $\lambda \geq 1$ , where  $C$  depends on  $u_0$  and  $\sigma$ , but not on  $\lambda$ . We deduce, for any  $t \in [0, T]$ :

$$(A.6) \quad \begin{aligned} \|Au\|_{L_t^q(L^r)} &\leq C_r \|Au_0\|_{L^2} \\ &\quad + C T^{2\sigma/k} \left( \lambda^{\frac{\sigma}{\sigma+1}} \|\nabla_x u\|_{L_t^\infty(L^2)}^{4\sigma/s} + 1 \right) \|Au\|_{L_t^q(L^r)}. \end{aligned}$$

Now assume that (2.4) is satisfied for some  $\varepsilon$  to be fixed later. Then by continuity (see Proposition 2.1), there exists  $\tau > 0$  such that

$$(A.7) \quad T^{2-(n-2)\sigma} \left( \lambda^{2\sigma} \|\nabla_x u\|_{L_t^\infty(L^2)}^{4\sigma} + 1 \right) \leq (2^{4\sigma} + 1) \varepsilon,$$

for  $0 \leq t \leq \tau$ . Choosing  $0 < \varepsilon \leq \varepsilon_0(n, \sigma)$ , the last term of (A.6) can be absorbed by the left hand side for  $0 \leq t \leq \tau$ :

$$\|Au\|_{L_t^q(L^r)} \leq 2C_r \|Au_0\|_{L^2}.$$

Strichartz inequalities and the above estimate yield, for  $t \in [0, T]$  such that (A.7) holds:

$$\begin{aligned} \|Au\|_{L_t^\infty(L^2)} &\leq \|Au_0\|_{L^2} + CT^{2\sigma/k} \left( \lambda^{\frac{\sigma}{\sigma+1}} \|\nabla_x u\|_{L_t^\infty(L^2)}^{4\sigma/s} + 1 \right) \|Au\|_{L_t^q(L^r)} \\ &\leq \|Au_0\|_{L^2} + C'T^{2\sigma/k} \left( \lambda^{\frac{\sigma}{\sigma+1}} \|\nabla_x u\|_{L_t^\infty(L^2)}^{4\sigma/s} + 1 \right) \|Au_0\|_{L^2}. \end{aligned}$$

By the conservation of mass, this estimate is interesting only when  $A = \nabla_x$ . Up to choosing  $\varepsilon$  even smaller, we see that as long as (A.7) is satisfied:

$$\|\nabla_x u\|_{L_t^\infty(L^2)} \leq 2 \|\nabla_x u_0\|_{L^2}.$$

Now suppose that (A.7) is not satisfied for  $t = T$ : there exists a minimal time  $t^* < T$  such that

$$\begin{aligned} T^{2-(n-2)\sigma} \left( \lambda^{2\sigma} \|\nabla_x u\|_{L_{t^*}^\infty(L^2)}^{4\sigma} + 1 \right) &= (2^{4\sigma} + 1) \varepsilon, \\ \|\nabla_x u\|_{L_{t^*}^\infty(L^2)} &\leq 2 \|\nabla_x u_0\|_{L^2}. \end{aligned}$$

The latest inequality yields, along with (2.4):

$$T^{2-(n-2)\sigma} \left( \lambda^{2\sigma} \|\nabla_x u\|_{L_{t^*}^\infty(L^2)}^{4\sigma} + 1 \right) \leq T^{2-(n-2)\sigma} (\lambda^{2\sigma} 2^{4\sigma} \|\nabla_x u_0\|_{L^2}^{4\sigma} + 1) \leq 2^{4\sigma} \varepsilon.$$

This contradicts the definition of  $t^*$ . Therefore, (A.7) is satisfied for  $t = T$ , which completes the proof of Corollary 2.2.

**A.3. Proof of Proposition 2.4.** For  $\alpha \in \mathbb{R}$ , define:

$$J_\alpha(t) = x + 2i(t - \alpha)\nabla_x = 2i(t - \alpha)e^{i\frac{|x|^2}{4(t-\alpha)}} \nabla_x \left( e^{-i\frac{|x|^2}{4(t-\alpha)}} \right).$$

Denote

$$\phi(t) = h(t)^{n\sigma-2} = \left( 1 - \frac{t}{a} \right)^{n\sigma-2}.$$

Besides the conservations of mass for  $u$  and  $v$ , and of energy for  $u$ , we have the following evolution laws:

$$\begin{aligned} \frac{d}{dt} \left( \|J_\alpha(t)u\|_{L^2}^2 - 4\frac{(t-\alpha)^2}{\sigma+1} \|u(t)\|_{L^{2\sigma+2}}^{2\sigma+2} \right) &= 4\frac{n\sigma-2}{\sigma+1} (t-\alpha) \|u(t)\|_{L^{2\sigma+2}}^{2\sigma+2}; \\ \frac{d}{dt} \left( \|\nabla_x v(t)\|_{L^2}^2 - \frac{\phi(t)}{\sigma+1} \|v(t)\|_{L^{2\sigma+2}}^{2\sigma+2} \right) &= \frac{-\phi'(t)}{\sigma+1} \|v(t)\|_{L^{2\sigma+2}}^{2\sigma+2}; \\ \frac{d}{dt} \left( \|J_\alpha(t)v\|_{L^2}^2 - 4\frac{(t-\alpha)^2\phi(t)}{\sigma+1} \|v(t)\|_{L^{2\sigma+2}}^{2\sigma+2} \right) &= \\ &= 4\frac{n\sigma-2}{\sigma+1} (t-\alpha)\phi(t) \|v(t)\|_{L^{2\sigma+2}}^{2\sigma+2} - \frac{4}{\sigma+1} (t-\alpha)^2\phi'(t) \|v(t)\|_{L^{2\sigma+2}}^{2\sigma+2}. \end{aligned}$$

**Lemma A.3.** *Let  $u_0 \in \Sigma$ ,  $2/n \leq \sigma < 2/(n-2)$  and  $T > 0$ . The following assertions are equivalent:*

- (1)  $u$  blows up at time  $T$ .
- (2)  $\|\nabla_x u(t)\|_{L^2} \rightarrow +\infty$  as  $t \rightarrow T$ .
- (3)  $\|u(t)\|_{L^{2\sigma+2}} \rightarrow +\infty$  as  $t \rightarrow T$ .
- (4) For any  $\alpha \neq T$ ,  $\|J_\alpha(t)u\|_{L^2} \rightarrow +\infty$  as  $t \rightarrow T$ .



*Proof of Lemma A.3.* The equivalence between the first two points follows from Proposition 2.1. The second point is equivalent to the third one by conservation of the energy.

For  $\alpha \neq T$ , Gagliardo–Nirenberg inequalities and the second writing for  $J_\alpha$  yield:

$$\|u(t)\|_{L^{2\sigma+2}}^{2\sigma+2} \leq \frac{C(n, \sigma)}{|t - \alpha|^{n\sigma}} \|u(t)\|_{L^2}^{2-(n-2)\sigma} \|J_\alpha(t)u\|_{L^2}^{n\sigma}.$$

We infer (3) $\Rightarrow$ (4) by the conservation of mass. Finally, if  $\|u(t)\|_{L^{2\sigma+2}}$  remains bounded as  $t \rightarrow T$ , then integrating the first evolution law above shows that  $\|J_\alpha(t)u\|_{L^2}$  remains bounded as  $t \rightarrow T$ .  $\square$

A similar result holds for  $v$ . Notice that if  $a > 0$ , then for  $0 < t < a$ ,  $\phi$  is smooth (bounded) and does not cancel. If  $a < 0$ , the same holds in a compact of  $\mathbb{R}_+$ .

**Lemma A.4.** *Let  $u_0 \in \Sigma$ ,  $2/n \leq \sigma < 2/(n-2)$  and  $T > 0$ , with  $T < a$  if  $a > 0$ . The following assertions are equivalent:*

- (1)  *$v$  blows up at time  $T$ .*
- (2)  *$\|\nabla_x v(t)\|_{L^2} \rightarrow +\infty$  as  $t \rightarrow T$ .*
- (3)  *$\|v(t)\|_{L^{2\sigma+2}} \rightarrow +\infty$  as  $t \rightarrow T$ .*
- (4) *For any  $\alpha \neq T$ ,  $\|J_\alpha(t)v\|_{L^2} \rightarrow +\infty$  as  $t \rightarrow T$ .*

*Proof.* The equivalence between (1) and (2) follows like for Proposition 2.1, since  $\phi$  is bounded from above and from below by positive constants.

The other equivalences follow like above, thanks to Gagliardo–Nirenberg inequalities.  $\square$

Then Proposition 2.4 follows from Lemma A.4 and the identity:

$$\|J_a(t)v\|_{L^2} = 2 \left\| \nabla_x u \left( \frac{at}{a-t} \right) \right\|_{L^2}.$$

**A.4. Proof of Proposition 2.6.** It consists of a slight adaptation of the proof of Proposition 2.1. Considering (2.10), the analog of (A.4) yields:

$$\begin{aligned} \|A(F(u))\|_{L_T^\infty(L^2)} &\leq \|Au_0\|_{L^2} + C\lambda \left\| e^{-2\sigma\delta t} A(|u|^{2\sigma}u) \right\|_{L_T^{q'}(L^{r'})} \\ &\leq \|Au_0\|_{L^2} + C\lambda \left\| e^{-\delta t} u \right\|_{L_T^k(L^s)}^{2\sigma} \|Au\|_{L_T^q(L^r)}, \end{aligned}$$

where the notation  $L_T^p$  now stands for  $L^p([0, T])$ . Using Gagliardo–Nirenberg inequality, we have:

$$\left\| e^{-\delta t} u \right\|_{L_T^k(L^s)} \leq C \left\| e^{-\delta t} \right\|_{L_T^k} \|u\|_{L_T^\infty(L^2)}^{1-\delta(s)} \|\nabla_x u\|_{L_T^\infty(L^2)}^{\delta(s)}.$$

Mimicking the proof of Proposition 2.1, we can apply a fixed point argument provided that:

$$\left\| e^{-\delta t} \right\|_{L_T^k} R_{\text{Id}}^{1-\delta(s)} R_{\nabla_x}^{\delta(s)} \ll 1.$$

This property is a consequence of the stronger one:

$$R_{\text{Id}}^{1-\delta(s)} R_{\nabla_x}^{\delta(s)} \ll \delta,$$

which is the condition stated in Proposition 2.6, whose proof is now complete.

*Remark.* This proof yields similar results for a larger class of damping. For  $\delta > 0$  and  $F \in L^1(\mathbb{R}_+)$  a positive function, define:

$$H(t, \delta) = -\delta \frac{F'(\delta t)}{F(\delta t)}.$$

Then for  $\delta$  satisfying (2.11) with another constant  $C$  (depending of  $F$ ), the solution of

$$i\partial_t \psi + \Delta \psi = -|\psi|^{2\sigma} \psi - iH(t, \delta) \psi, \quad x \in \mathbb{R}^n \quad ; \quad \psi|_{t=0} = u_0,$$

does not blow up in the future. In Prop. 2.6, we considered the case  $F(y) = e^{-y}$ . Considering  $F(y) = (1 + y)^{-\alpha}$  with  $\alpha > 1$  yields a damping function

$$H(t, \delta) = \alpha \frac{\delta}{1 + \delta t},$$

which goes to zero as  $t \rightarrow +\infty$ . Even though the damping is less and less strong, (2.11) ensures global existence in  $H^1$  in the future.

## REFERENCES

- [1] W. Bao, S. Jin, and P. A. Markowich, *Numerical study of time-splitting spectral discretizations of nonlinear Schrödinger equations in the semiclassical regimes*, SIAM J. Sci. Comput. **25** (2003), no. 1, 27–64.
- [2] W. Bao, N.J. Mauser, and H.P. Stimming, *Effective one particle quantum dynamics of electrons: a numerical study of the Schrödinger-Poisson- $X\alpha$  model*, Comm. Math. Sci. **1** (2003), no. 4, 809–831.
- [3] C. Besse, *A relaxation scheme for the nonlinear Schrödinger equation*, SIAM J. Numer. Anal. **42** (2004), no. 3, 934–952.
- [4] C. Besse, B. Bidégaray, S. Descombes, *Order estimates in time of the splitting methods for the nonlinear Schrödinger equation*, SIAM J. Numer. Anal. **40**, No. 1 (2002), 26–40
- [5] C. Besse, N. J. Mauser, and H. P. Stimming, *Numerical study of the Davey-Stewartson system*, M2AN Math. Model. Numer. Anal. **38** (2004), no. 6, 1035–1054.
- [6] J. Bourgain, *Global solutions of nonlinear Schrödinger equations*, American Mathematical Society Colloquium Publications, vol. 46, American Mathematical Society, Providence, RI, 1999.
- [7] J. Bourgain and W. Wang, *Construction of blowup solutions for the nonlinear Schrödinger equation with critical nonlinearity*, Ann. Scuola Norm. Sup. Pisa Cl. Sci. (4) **25** (1997), no. 1-2, 197–215 (1998), Dedicated to Ennio De Giorgi.
- [8] T. Cazenave, *Semilinear Schrödinger equations*, Courant Lecture Notes in Mathematics, vol. 10, New York University Courant Institute of Mathematical Sciences, New York, 2003.
- [9] T. Cazenave and F. Weissler, *Rapidly decaying solutions of the nonlinear Schrödinger equation*, Comm. Math. Phys. **147** (1992), 75–100.
- [10] P. Donnat, J.-L. Joly, G. Métivier, and J. Rauch, *Diffraction nonlinear geometric optics*, Séminaire sur les Équations aux Dérivées Partielles, 1995–1996, Exp. No. XVII, École Polytech., Palaiseau, 1996.
- [11] G. Fibich, *Self-focusing in the damped nonlinear Schrödinger equation*, SIAM J. Appl. Math. **61** (2001), no. 5, 1680–1705.
- [12] G. Fibich, N. Gavish and X.-P. Wang, *New singular solutions of the nonlinear Schrödinger equation*, Phys. D **211** (2005), no. 3-4, 193–220.
- [13] J. Ginibre and G. Velo, *Smoothing properties and retarded estimates for some dispersive evolution equations*, Comm. Math. Phys. **144** (1992), no. 1, 163–188.
- [14] R. T. Glassey, *On the blowing up of solutions to the Cauchy problem for nonlinear Schrödinger equations*, J. Math. Phys. **18** (1977), 1794–1797.

- [15] J.-L. Joly, G. Métivier, and J. Rauch, *Diffraction nonlinear geometric optics with rectification*, Indiana Univ. Math. J. **47** (1998), no. 4, 1167–1241.
- [16] M. Keel and T. Tao, *Endpoint Strichartz estimates*, Amer. J. Math. **120** (1998), no. 5, 955–980.
- [17] Y. Martel, *Blow-up for the nonlinear Schrödinger equation in nonisotropic spaces*, Nonlinear Anal. **28** (1997), no. 12, 1903–1908.
- [18] F. Merle, *Construction of solutions with exactly  $k$  blow-up points for the Schrödinger equation with critical nonlinearity*, Comm. Math. Phys. **129** (1990), no. 2, 223–240.
- [19] F. Merle, *Determination of blow-up solutions with minimal mass for nonlinear Schrödinger equations with critical power*, Duke Math. J. **69** (1993), no. 2, 427–454.
- [20] F. Merle and P. Raphaël, *On universality of blow-up profile for  $L^2$  critical nonlinear Schrödinger equation*, Invent. Math. **156** (2004), no. 3, 565–672.
- [21] F. Merle and P. Raphaël, *Profiles and quantization of the blow up mass for critical nonlinear Schrödinger equation*, Comm. Math. Phys. **253** (2005), no. 3, 675–704.
- [22] H. Nawa, *Asymptotic and limiting profiles of blowup solutions of the nonlinear Schrödinger equation with critical power*, Comm. Pure Appl. Math. **52** (1999), no. 2, 193–270.
- [23] T. Ogawa and Y. Tsutsumi, *Blow-up of  $H^1$  solution for the nonlinear Schrödinger equation*, J. Differential Equations **92** (1991), no. 2, 317–330.
- [24] G. Perelman, *On the formation of singularities in solutions of the critical nonlinear Schrödinger equation*, Ann. Henri Poincaré **2** (2001), no. 4, 605–673.
- [25] V. M. Pérez-García and X. Liu, *Numerical methods for the simulation of trapped nonlinear Schrödinger systems*, Appl. Math. Comput. **144** (2003), no. 2-3, 215–235.
- [26] P. Raphaël, *Stability of the log-log bound for blow up solutions to the critical nonlinear Schrödinger equation*, Math. Ann. **331** (2005), no. 3, 577–609.
- [27] P. Raphaël, *Sur la dynamique explosive des solutions de l'équation de Schrödinger non linéaire*, Séminaire: Équations aux Dérivées Partielles 2004–2005, Exp. No. III, École polytech., Palaiseau.
- [28] C. Sulem and P.-L. Sulem, *The nonlinear Schrödinger equation, self-focusing and wave collapse*, Springer-Verlag, New York, 1999.
- [29] M. I. Weinstein, *Nonlinear Schrödinger equations and sharp interpolation estimates*, Comm. Math. Phys. **87** (1982/83), no. 4, 567–576.
- [30] M. I. Weinstein, *On the structure and formation of singularities in solutions to nonlinear dispersive evolution equations*, Comm. in Partial Diff. Eq. **11** (1986), no. 5, 545–565.
- [31] K. Yajima, *Existence of solutions for Schrödinger evolution equations*, Comm. Math. Phys. **110** (1987), 415–426.
- [32] V. E. Zakharov and A. B. Shabat, *Exact theory of two-dimensional self-focusing and one-dimensional self-modulation of waves in nonlinear media*, vZ. Èksper. Teoret. Fiz. **61** (1971), no. 1, 118–134.

(C. Besse) SIMPAF TEAM – INRIA FUTURS, LABORATOIRE PAUL PAINLEVÉ, UMR CNRS 8524, UNIVERSITÉ DES SCIENCES ET TECHNOLOGIES DE LILLE, CITÉ SCIENTIFIQUE, 59655 VILLENEUVE D'ASCQ CEDEX, FRANCE

*E-mail address:* Christophe.Besse@math.univ-lille1.fr

(R. Carles) MAB, UMR CNRS 5466, UNIVERSITÉ BORDEAUX 1, 351 COURS DE LA LIBÉRATION, 33405 TALENCE CEDEX, FRANCE

*E-mail address:* Remi.Carles@math.cnrs.fr

(N. J. Mauser) WOLFGANG PAULI INSTITUTE C/O FAK. F. MATH., UNIVERSITÄT WIEN, NORDBERGSTR. 15, A 1090 WIEN, AUSTRIA

*E-mail address:* mauser@courant.nyu.edu

(H. P. Stimming) WOLFGANG PAULI INSTITUTE AND FAKULTÄT F. MATH., UNIVERSITÄT WIEN, NORDBERGSTR. 15, A 1090 WIEN, AUSTRIA

*E-mail address:* hans.peter.stimming@univie.ac.at